

H SAF-GPM collaboration activity: assessment of GMI snowfall detection capabilities based on synergistic CloudSat observations (and the new PNPR for GMI)

Giulia Panegrossi

Paolo Sanò, Anna Cinzia Marra, Jean-François Rysman, Daniele Casella*
and Stefano Dietrich
CNR-ISAC, Rome, Italy

(Now at SERCO S.p.A, Frascati, Italy)*

in collaboration with

Ben Johnson

UCAR/JCSDA, NOAA, College Park MD, USA

Mark Kulie

Michigan Technological University, Houghton, MI, USA

EUMETSAT SAF on Support to Operational Hydrology and Water Management

<http://hsaf.meteoam.it>

established in 2005 – CDOP-2 (2012-2017) - **New phase: CDOP-3 (2017-2022)**

Role of CNR-ISAC

development and delivery of precipitation products:

- 1) Exploitation of current and future PMW radiometers (conically and cross-track scanning) on board LEO satellites, offering the most complete set of satellite based observations to retrieve surface precipitation; **ESP-SG MWS MWI day-1 products in CDOP-3**
- 2) Combination of LEO MW estimates and GEO IR observations for NRT precipitation monitoring and hydrological applications to benefit from physical robustness of MW and space/time resolution of IR. **MTG-based products in CDOP-3**

“Bridge science and research into development and operations”

(Cit. L. Shuller, Manager of the EUMETSAT SAF Network)

EUMETSAT SAF on Support to Operational Hydrology and Water Management

<http://hsaf.meteoam.it>

established in 2005 – CDOP-2 (2012-2017) - **New phase: CDOP-3 (2017-2022)**

*No-cost collaboration proposal
approved in 2014 by the NASA PMM Research Program*

“H-SAF and GPM: precipitation algorithm development and validation activity”

Long term collaboration between EUMETSAT H SAF and GPM on:

- **precipitation retrieval algorithm development**, interaction on several critical aspects of interest both to H SAF and GPM; **Scientific coordinator: Giulia Panegrossi (ISAC-CNR)**
- **validation activity**, through the connection between the well established H-SAF product validation and hydrological validation programs and the Ground Validation/Calibration activity of GPM; **Scientific Coordinator: Silvia Puca (DPC)**

(Next to) Poster #205

DPR products (V04 vs. V05): validation over Italy using 2015-2016 quality-controlled data from the Italian radar network

H SAF PMW Precipitation rate products in CDOP-2 (2012-2017): exploitation of GPM constellation

Product ID (Instrument)	Product Description	Algorithm	Currently available satellites	Status/ Availability
H01 (SSMIS)	Precipitation rate at ground by MW conical scanner SSMIS (MSG full disk)	Physically-based Bayesian CDRD	DMSP F16/F17/F18 (F19)	Operational
H02A/B (AMSU/ MHS)	Precipitation rate at ground by MW cross-track scanners AMSU/MHS (A: H-SAF area / B: MSG full disk)	Neural Network PNPR	MetOp-A/B NOAA-18/19 (MetOp-C)	A: Operational B: Pre-Op.(expected Op. Q1-Q2 2018)
H18 (ATMS)	Precipitation rate at ground by MW cross-track scanners ATMS (MSG full disk)	Neural Network PNPR	Suomi NPP (JPSS)	Exp. Op. Q1-Q2 2018
H17 (AMSR-2)	Precipitation rate at ground by MW conical scanner AMSR-2 (MSG full disk)	Physically-based Bayesian CDRD	GCOM W1	Auxiliary: Support to MW-only and MW/IR combined products
H19 (GMI)	Precipitation Rate at ground by conical scanner GMI (MSG full disk)	Physically-based Bayesian CDRD	GPM	Auxiliary: Support to MW-only and MW/IR combined products
H20 (GMI)	Precipitation Rate at ground by GMI – (GMI/DPR Observational Dataset) (Global)	Neural Network	GPM	Auxiliary: Support to MW-only and MW/IR combined products

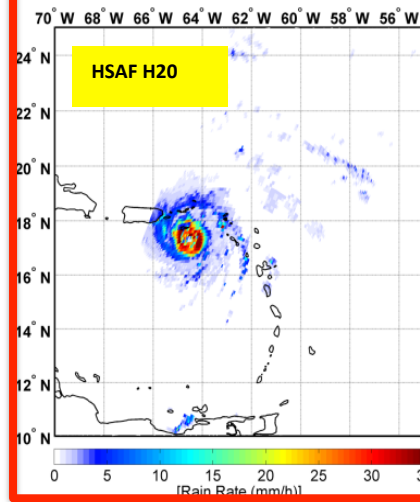
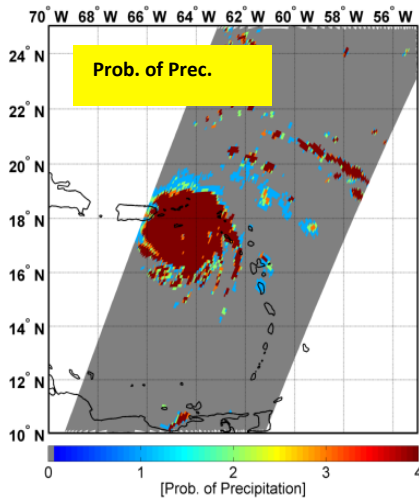
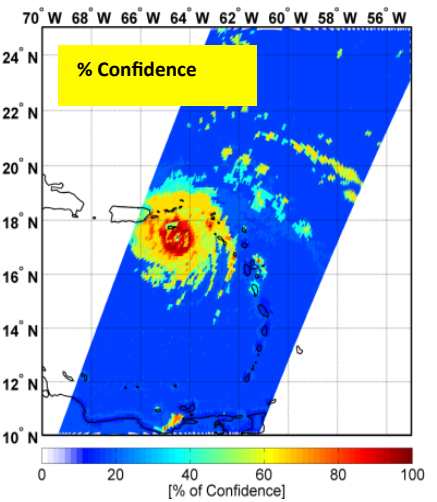
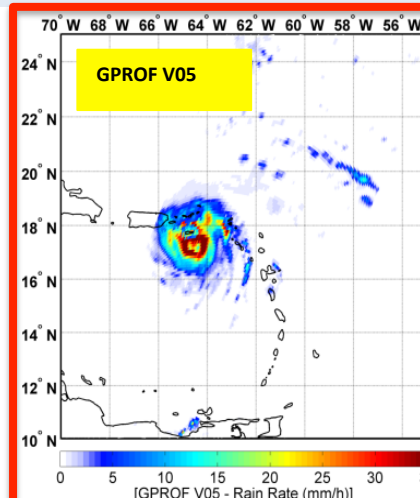
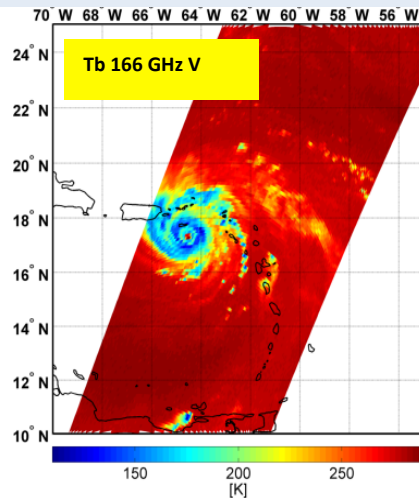
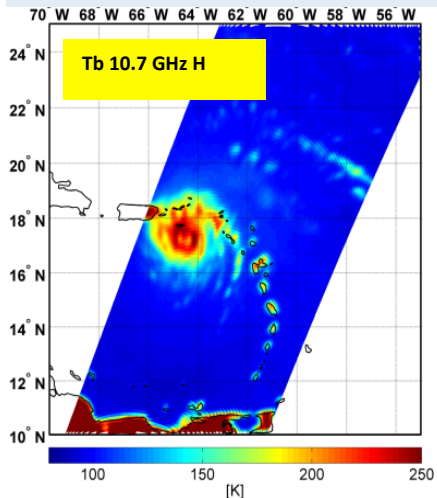
The new Global PNR for GMI (H2O)

Passive microwave Neural network Precipitation Retrieval (PNR) (Sanò et. Al., 2015, 2016, AMT) applied to GMI

Training Dataset: GMI/DPR V04 (2B-CMB) 01/04/2014 – 08/06/2016 (50x10⁶ rain, 150x10⁶ no rain).

Area: GPM Global Area (Lon: 180°W - 180°E, Lat: 68°S - 68° N)

- 1 PCA approach: a) **different blocks of channels**; b) **contribution of PCs in each block depending on surface background**;
- 2 **Combined PCs and TB-derived variables** (e.g. TB differences)
- 4 **Selection of ancillary parameters** (TPW, T2m, reanalysis 2011-2016 period).
- 5 Design and training of **on unique final ANN** [Cross Validation (CV) method].



Hurricane Maria 20 September, 2017 02:03UTC

In addition to the **surface precipitation (mm/h)**, the HSAF H2O product provides

- **Percentage of Confidence Index;**
- **Precipitation probability index**

HSAF H2O product

- shows a good agreement with GPROF V05 in terms of precipitation pattern;
- lower precipitation rates than GPROF moving away from the center of the hurricane.

The new Global PNPR for GMI (H2O)

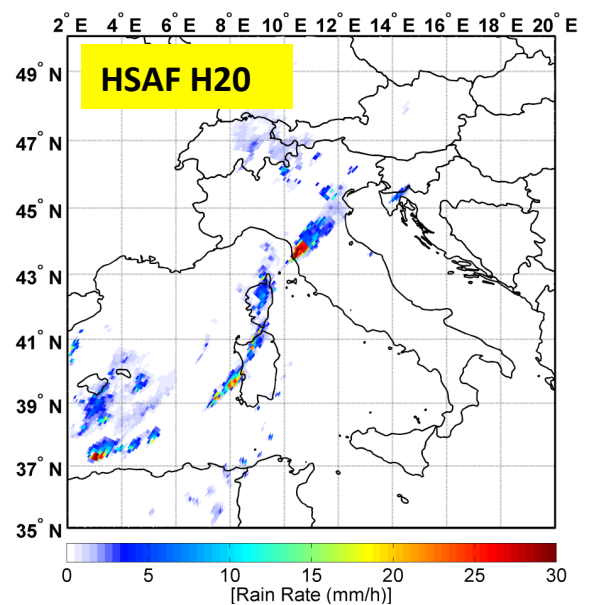
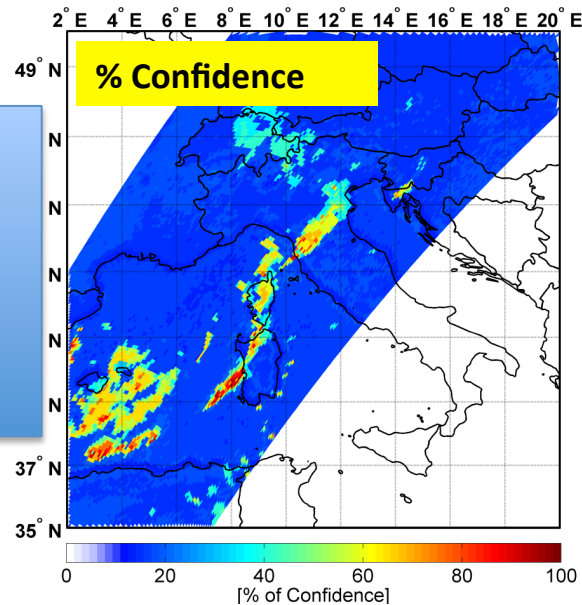
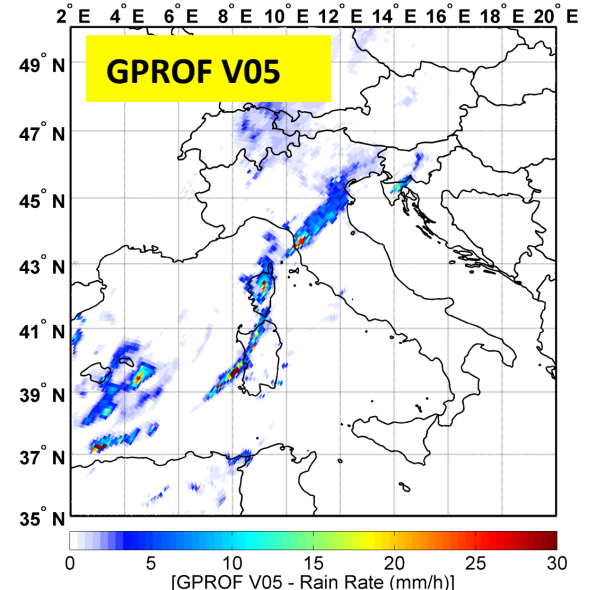
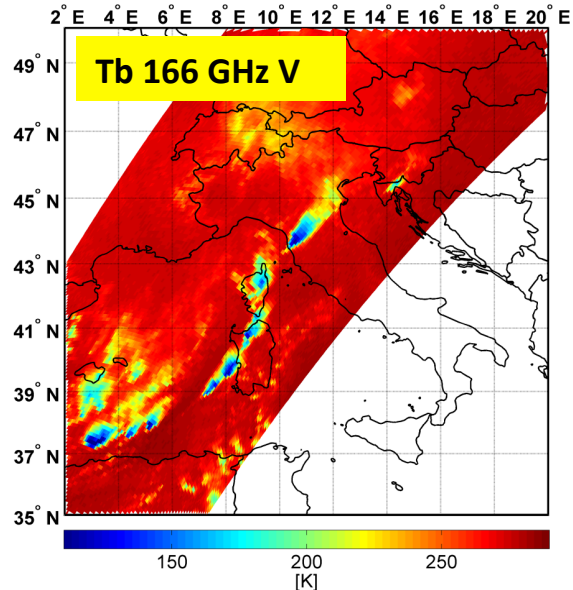
Flash Flood Livorno
(Tuscany) Italy

GMI overpass
10 September 2017
01:17 UTC

(Next to) Poster #205

Wednesday

*Validation of GPROF V05
and comparison with H2O
over Italy*



H SAF Federated Activity FA_15_01

with PMM Science Team members:

Mark Kulie (MTU), and Ben Johnson (UCAR/JCSDA, NOAA)

Cooperation on the use of combined spaceborne active and passive MW observations for precipitation retrieval

Main goal: Prepare and exploit datasets from coincident overpasses of spaceborne precipitation radars [**GPM DPR and CloudSat CPR**] and PMW radiometers for the refinement and development of precipitation retrieval techniques **with focus on snowfall**

- **GPM-DPR vs. CloudSat CPR:** Evaluation of DPR capabilities to observe snowfall with respect to CPR, assessment of global snowfall mass estimate by DPR vs. CPR;
- Investigation on the limitations and capabilities of ATMS and **GMI to observe snowfall using coincident CloudSat CPR measurements**

CloudSat-based assessment of GMI snowfall detection capabilities

(Panegrossi et al., Remote Sensing, submitted)

Motivations

- You et al. (2016) analyzed a coincident **GPM-DPR database** to determine optimal channel combinations for snowfall detection over land;
- Ebtehaj and Kummerow (2017) analyze in detail the GMI channel response to snowfall, using **DPR products as reference**;
- Gong et al. (2017) analyze global 166 GHz (vs. 89 GHz) polarization signature and find that **at high latitudes the relationship with precipitation is quite complex and requires a separate analysis**;
- Casella et al. (2017) showed that DPR detects 5-7% of the global snowfall events with respect to CloudSat CPR, while **29-34% of the global snowfall mass is correctly detected by DPR v4 products (see Poster #205 on Wednesday)**

Goal

Use of CloudSat CPR to **define the limitations and capabilities of GMI to observe snowfall and to study 166 GHz polarization signature at high latitudes** in relation to environmental characteristics (i.e., background surface, water vapor content), and to cloud properties (e.g., snow water path, presence of supercooled droplets)

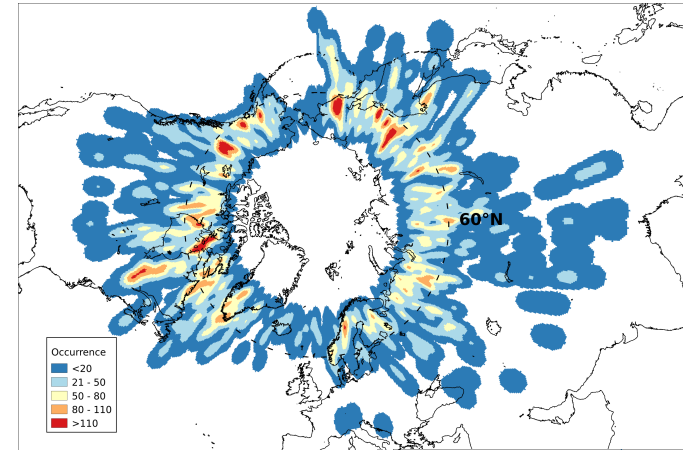
GMI/CPR snowfall dataset

Based on the NASA 2B-CSATGPM product (J. Turk)

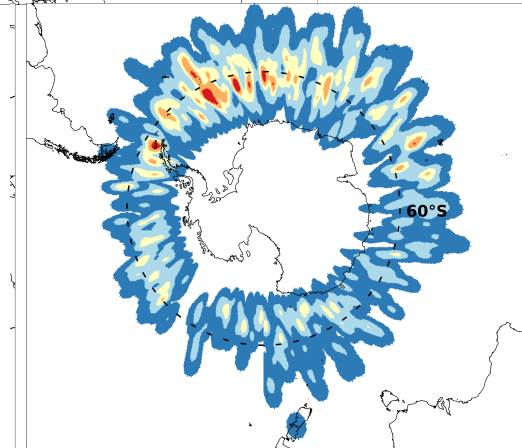
Period	03/14 - 5/16
Averaged pixels	529350
Snowfall Pixels	48194
Products	2B-CMB (V4 and V5) 2A-DPR (V4 and V5) 1C-GMI (V5) GMI 2B-GPROF (V4 and V5) 2C-SNOW-profile 2C-PRECIP-COLUMN 2B-CLOUD-CLASS Calipso/CPR DARDAR (ice cloud properties) ECMWF-AUX
Ancillary variables	T2m Surf Pres Specif. Hum. T500m TPW AMSR2 NOAA SNIDC (Sea ice)

Other variables related to the co-location/ averaging procedure are provided: minimum distance, mean distance, number of CPR pixels within GMI pixel.

GMI-CPR coincidences within 15 minute time interval;
 Dataset generated at GMI spatial resolution (high frequency channels)

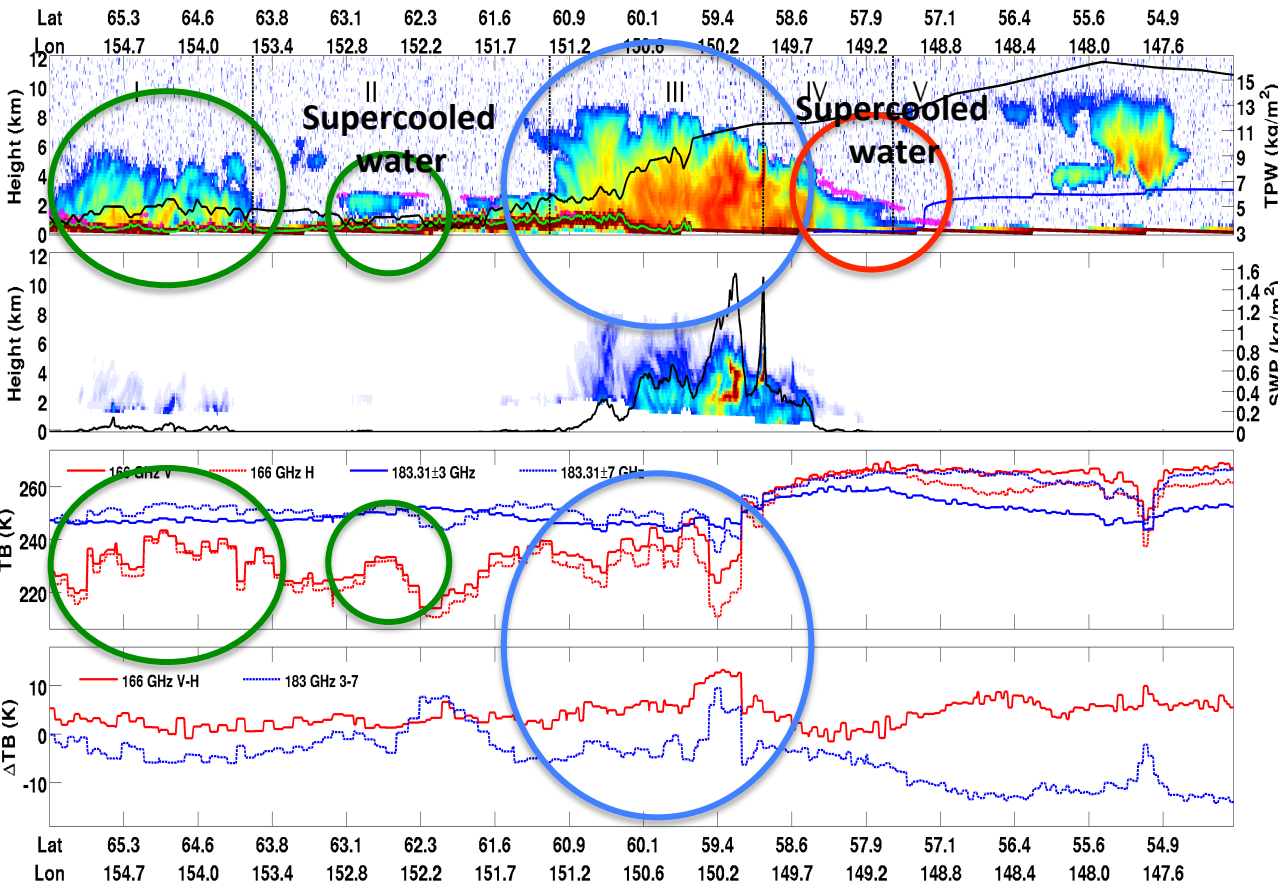


Number of occurrences of snowfall elements (indicated by the colors) in the Northern (left) and Southern (right) hemispheres.



Global distribution of snowfall elements in the GMI/CPR coincidence dataset (03/2014-5/2016).

Frontal snowfall event - Eastern Russia 30 April 2014

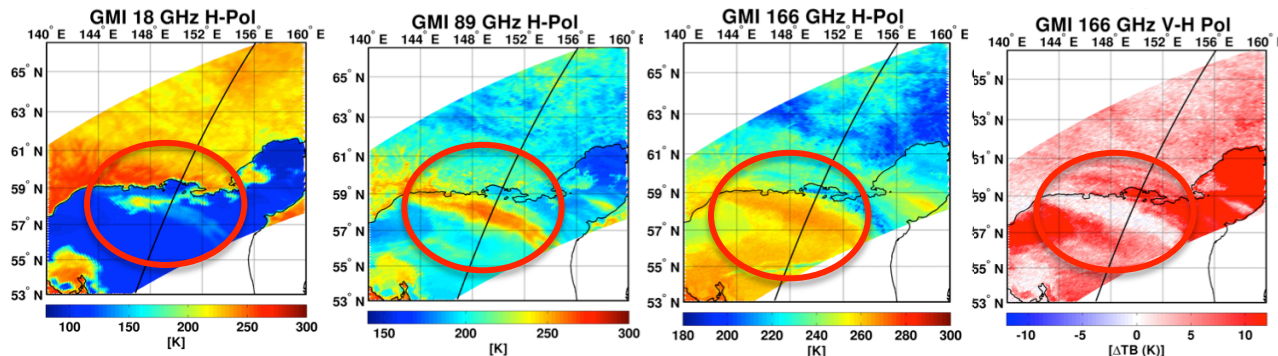


Land (cold and dry)
Sector III: Deeper snowfall segment; scattering effects at 166 GHz (and 183 GHz) (166 TB depression up to 30K); 166ΔTB up to 12 K due to polarization by oriented ice crystals

Sector I/II: Shallow/weak snow clouds; sensitivity of 166 GHz channels; 166 TBs increase with respect to clear sky related presence of CPR/CALIPSO supercooled water

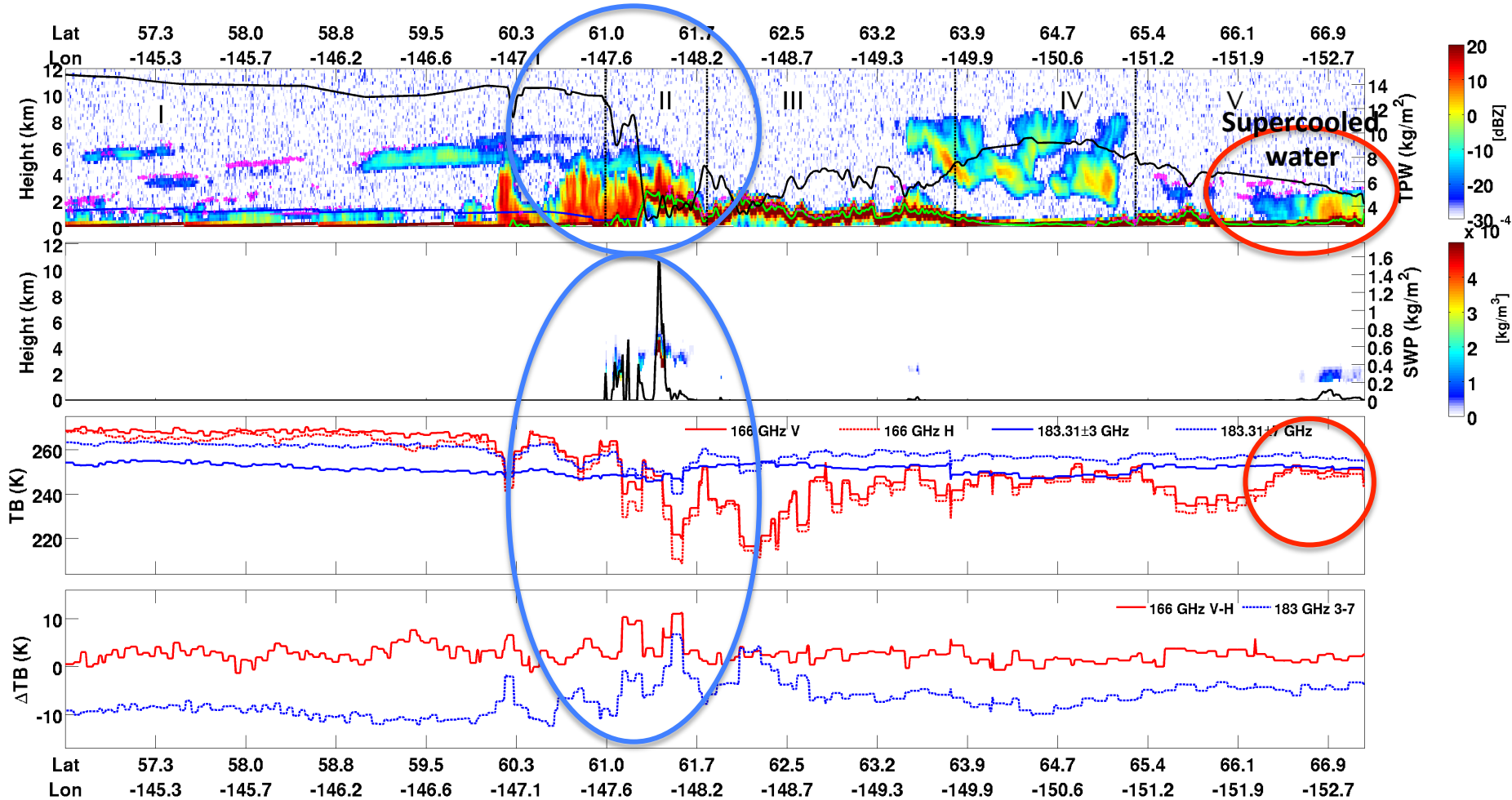
Ocean (moist and warmer)

Sector IV/V: Dampening effect of water vapor at 166 GHz; effect of supercooled droplets visible at 89 GHz; presence of low-level mixed phase precipitation (evident < 37 GHz. Upper level cloud associated to strong signal at 166 and 183 GHz



GMI TB maps at 18.7, 89 (H-pol) and 166 GHz (H-Pol), and 166 ΔTB ; black line indicates the CloudSat track

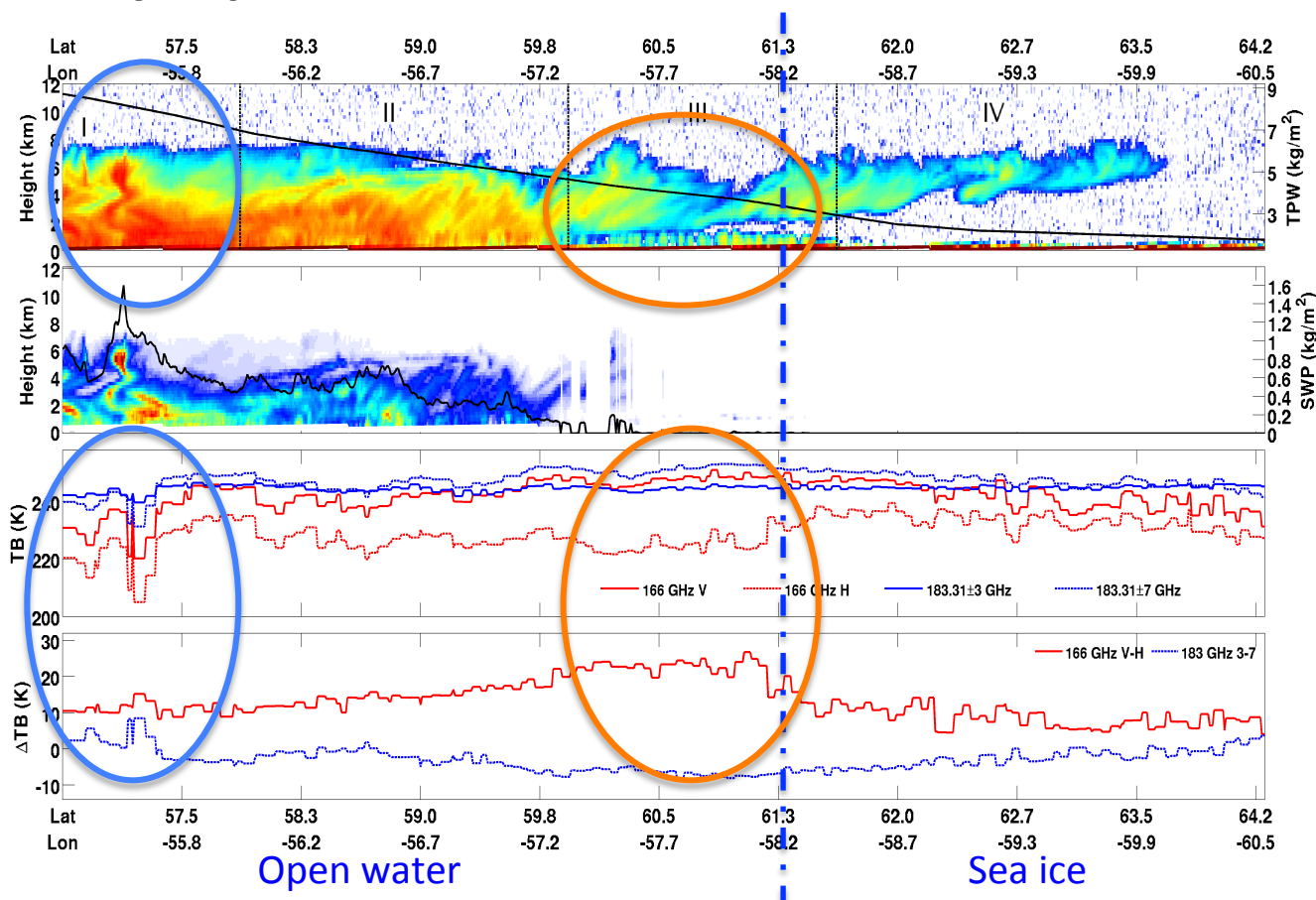
Orographic event on 14 December 2014 over Alaska



Sector II: Orographic snowfall segment; transition from moist to dry air; scattering effects at 166 GHz (and 183 GHz); 166ΔTB up to 10K due to polarization by oriented ice crystals

Sector V: Cold and dry conditions; Shallow/weak snow cloud; sensitivity of 166 GHz channels; 166 TBs increase with respect to clear sky (presence of CPR/CALIPSO supercooled water)

Synoptic snowfall event over the Labrador Sea on 27 March 2014



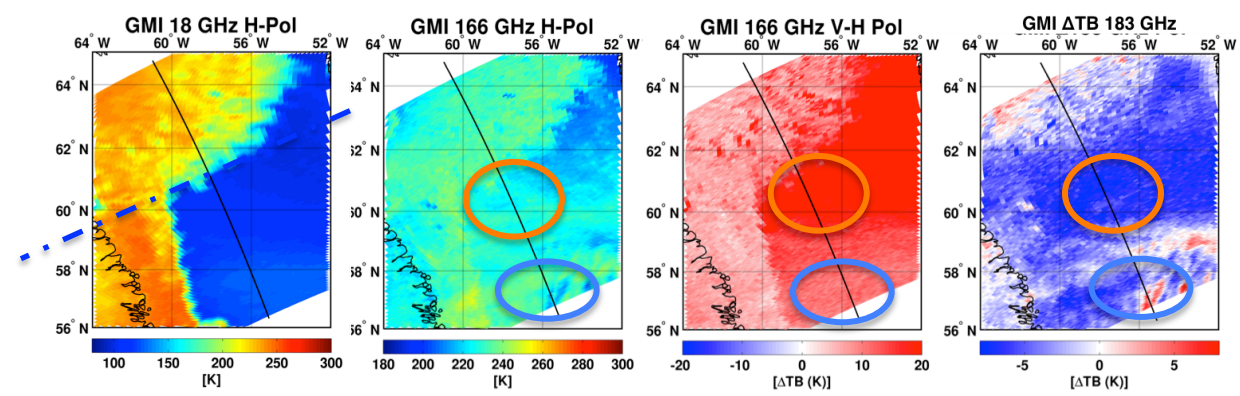
Sector I: Deep snow cloud, Z up to 10-15 dBZ, 166 Δ TB up to 10-15K; scattering effects at 166 GHz (and 183 GHz)

Sector III: multilayer cloud, with a very shallow snowfall layer (< 1 km thick, missed by 2C-SNOW); 166 Δ TB up to 20 K (surface+ice crystals)

Open water

Sea ice

TPW gradually decreases from 9 to < 2 kg/m²; transition from open water to sea ice around 61°N



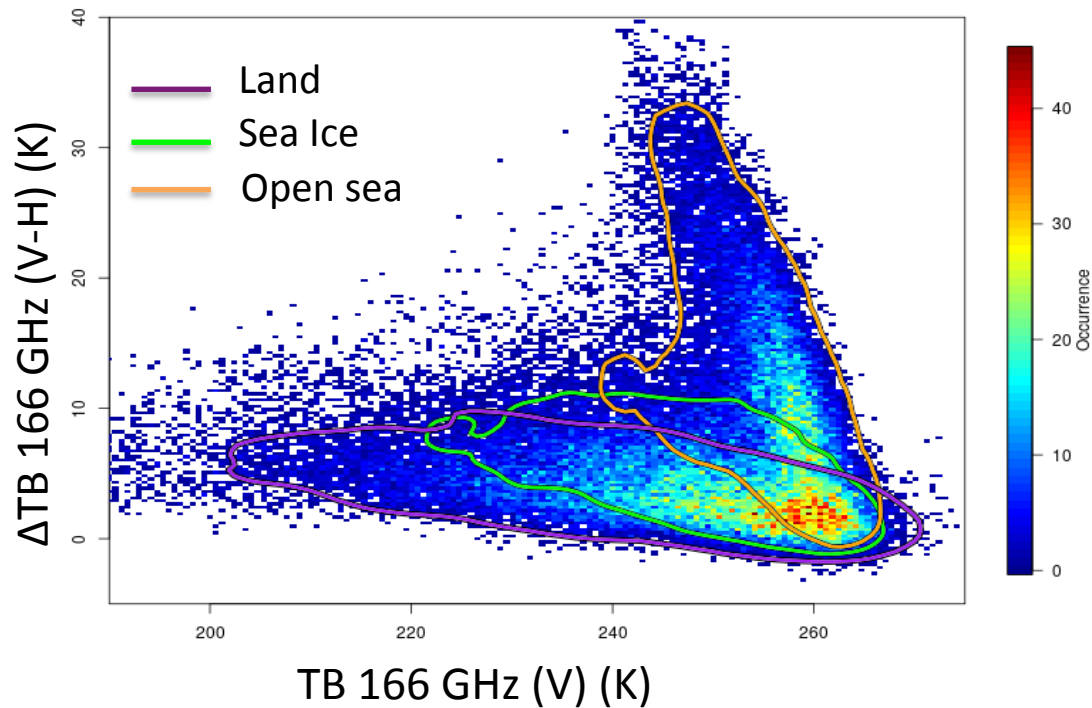
Analysis of the GMI/CPR global dataset: 166 GHz channels and snowfall (*high latitudes*)

Regression tree statistical analysis found good correlation between **166 Δ TB and SWP** for:

Land (88% below freezing):
TPW > 3.6 kg/m² IWP > 0.24 kg/m²

Sea Ice (SIC > 57%):
TPW > 5 kg/m²

Open water (SIC < 57%): low correlation because of predominant effect of the surface on 166 Δ TB



The 2-D histogram in 166 GHz Δ TB/TB space (200x100 bins) (*mean 166 Δ TB or TB value in each bin*);
Colorbar: % of occurrences. Contours: 90% occurrences in the 3 background surface manifolds

- Distinctive bell-shape (peaking near 166 Δ TB=10 K) is not found (e.g., Gong et al., 2017);
- Behavior similar to 89 GHz at lower latitudes (e.g., Gong et al., 2017) (low opacity of the atmosphere - low TPW);
- Different shape and range of 166 Δ TB values of the sea ice with respect to the open water; similarity to land;
- Different TB range for the three surfaces.

Analysis of GMI 166 GHz channels and CPR snowfall (high latitudes)

Open sea:

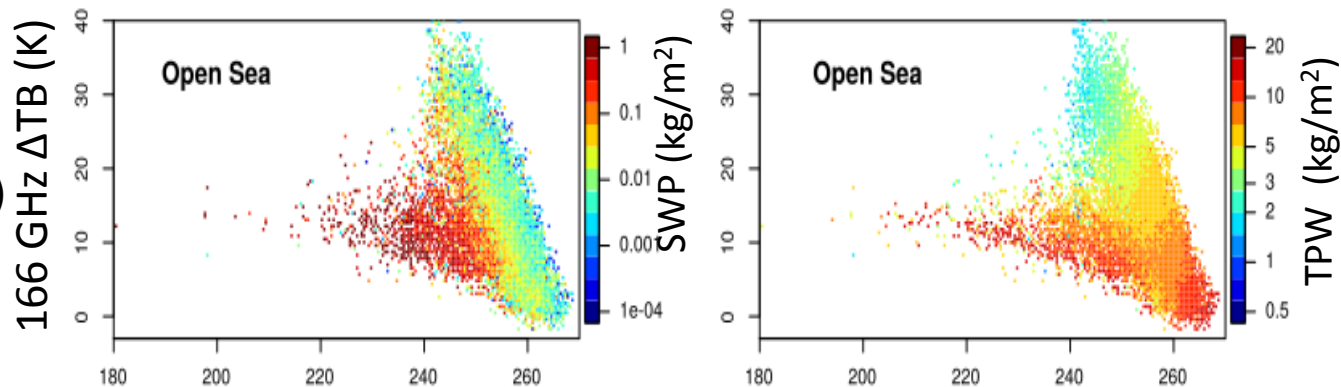
Two regimes:

1) $TPW < 10 \text{ kg/m}^2$ (low SWP):
linear relationships ΔTB vs.
TB;

2) $TPW > 10 \text{ kg/m}^2$ (high SWP)

TB ↓ as SWP ↑

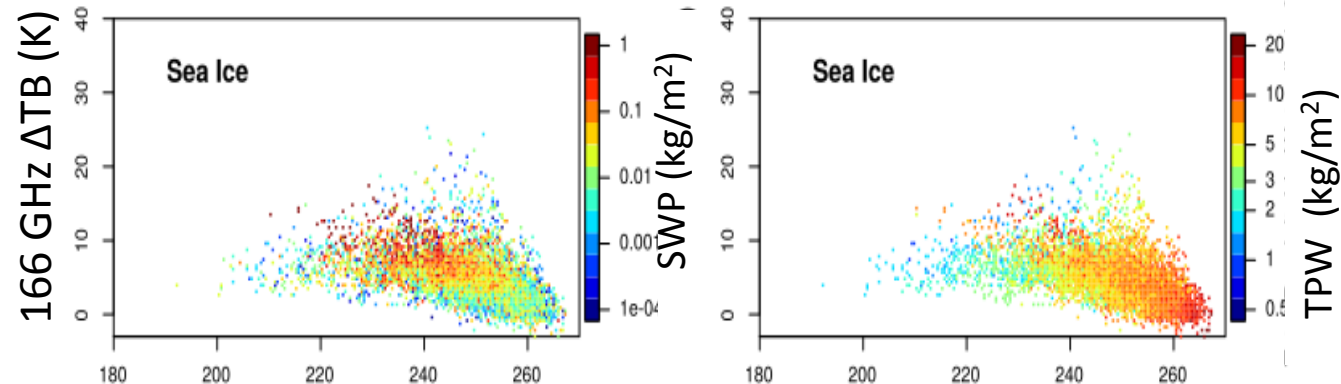
No dependence of ΔTB on
SWP



Sea ice: both ΔTB and TB
signal are related to the
SWP

ΔTB ↑ as SWP ↑

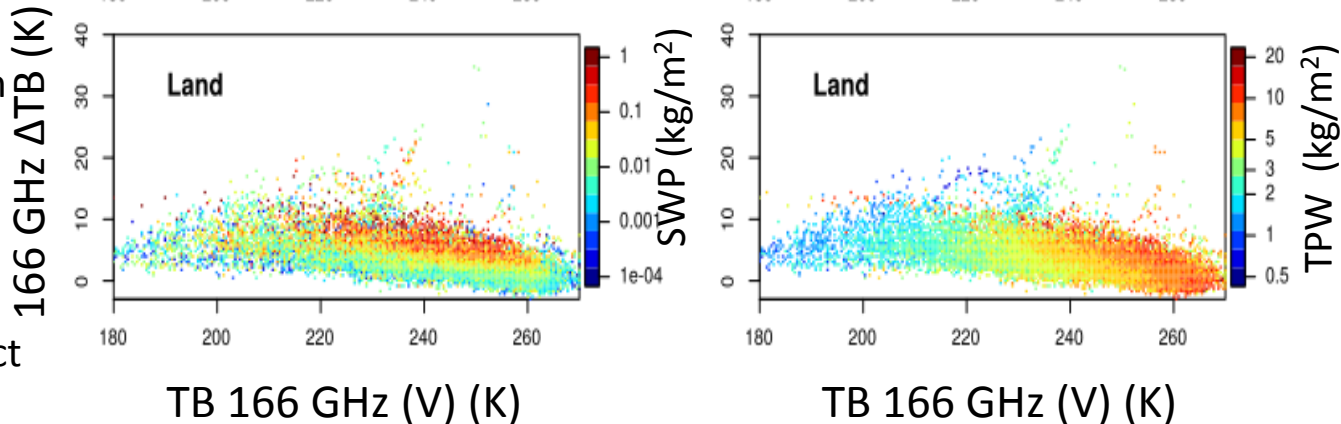
TB ↓ as SWP ↑



Land: no dependence of TB on
SPW

ΔTB ↑ as SWP ↑

(for $TPW > 3-4 \text{ kg m}^{-2}$)



[TB > 260K TPW dampens effect
of cloud (low SWP)]

TB 166 GHz (V) (K)

TB 166 GHz (V) (K)

Analysis of GMI/CPR snowfall dataset

Effect of supercooled droplets on TBs and ΔTB at 166 GHz

Classification based on CloudSat CPR and CALIPSO products

CS= clear sky

SN= snowfall only (SWP > 0 kg/m²)

SCE= snowfall and supercooled water within cloud

SCT= snowfall and supercooled water on top layer

Clear sky: Signal related to surface emission (and polarization) and to water vapor.

Over land, sharp variation for low TPW (polarization is visible)

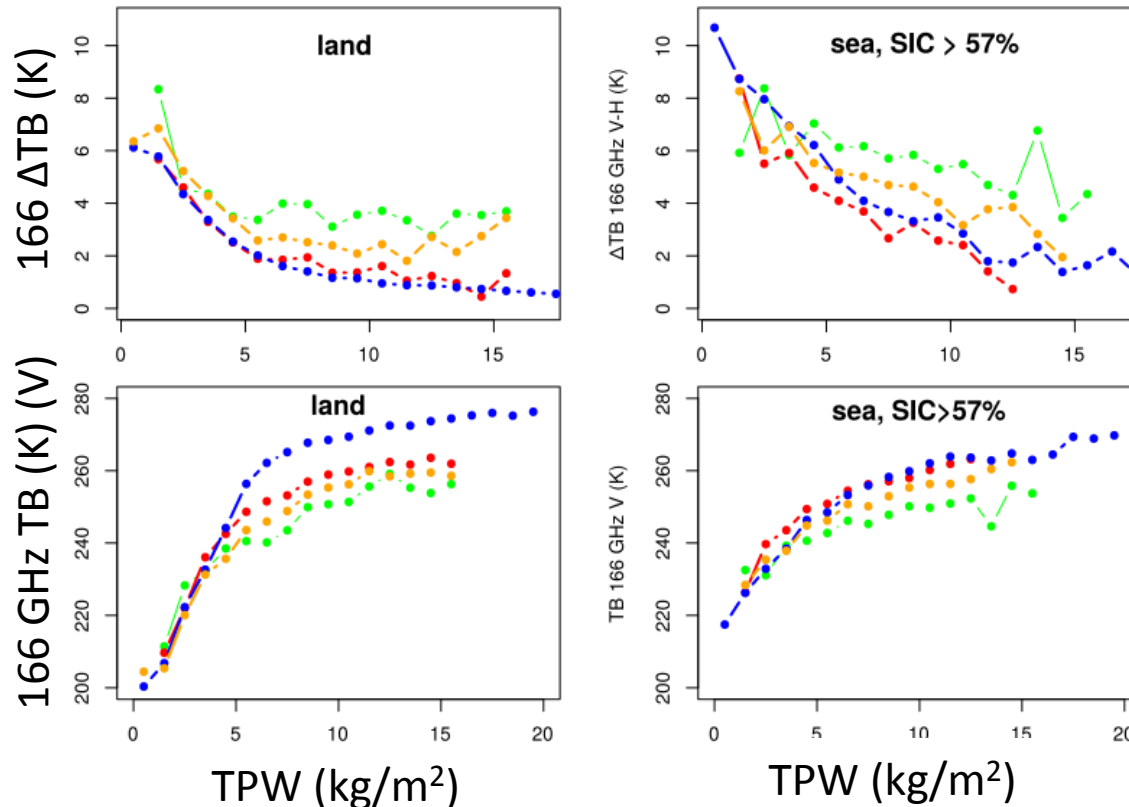
Snowfall: Distinct scattering and polarization signal by ice crystals with respect to CS.

Signal increases with TPW for:

TPW > 4 kg/m² over land

TPW > 5 kg/m² over sea ice

Supercooled water (on top and embedded in cloud): very strong impact on TBs and ΔTB (signal comparable to clear sky conditions when on top layer); **Tends to cancel the scattering effect and polarization due to the ice crystals**



Datasets are grouped based on surface type, and 21 TPW bins

Y-axis: **Median TB and ΔTB values** computed in each bin

Analysis of GMI/CPR snowfall dataset

Effect of supercooled droplets on TBs and ΔTB at 166 GHz

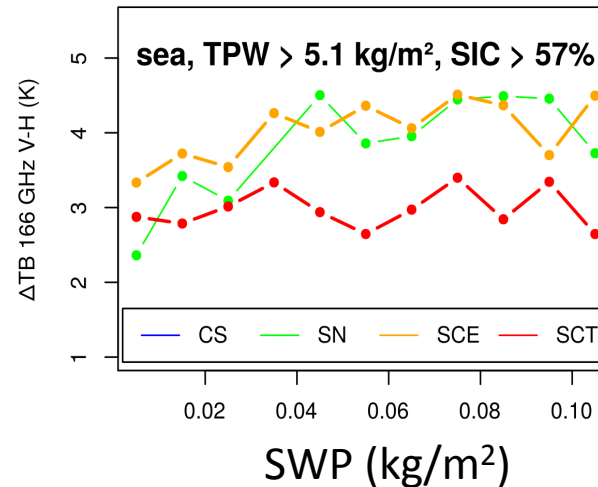
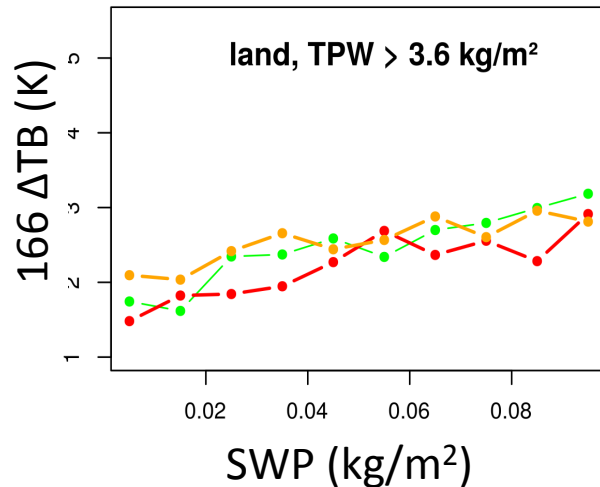
Classification based on CloudSat CPR and CALIPSO products

CS= clear sky

SN= snowfall only (SWP > 0 kg/m²)

SCE= snowfall and supercooled water within cloud

SCT= snowfall and supercooled water on top layer



In presence of snowfall ΔTB increases with SWP;

Over land the trend is maintained in presence of supercooled water, but ΔTB tends to be lower when on top layer (SCT) ;

Over sea ice trend is less visible for SWP > 0.05 kg/m²; supercooled water on top layer(SCT) may eliminate this trend and ΔTB is 40% lower

Datasets are grouped based on surface type, and 11 SWP bins

Y-axis: **Median ΔTB values** computed in each bin

Conclusions

Assessment of the potential of GMI high-frequency channels to detect snowfall at *high latitudes* using coincident CloudSat CPR (and CALIPSO) observations is complementary to previous studies. It defines some quantitative criteria and guidelines to build a GMI snowfall detection algorithm based on CloudSat.

- 1. Case Studies:** evidenced qualitatively the important interconnection of background surface characteristics, atmospheric water vapor content, and presence and vertical distribution of supercooled cloud water on GMI TB and Δ TB relation to snowfall and cloud properties.
- 2. Global Analysis of 166 GHz Δ TB and TB sensitivity to CPR snowfall:**
 - Regression tree statistical analysis was used to quantitatively define critical thresholds of various parameters (e.g., sea ice concentration (SIC), TPW, SWP) for the optimal use of the 166 GHz Δ TB for snowfall detection over land and over sea.
 - 166 GHz Δ TB, TB, and SWP relationship analysis for various surface types was used to define the conditions and the potentials of the 166 GHz channel relation to snowfall at high latitudes, and impact of supercooled cloud droplets.

- **New snowfall detection algorithm based on GMI/CPR coincidence dataset (see Poster #205 on Wednesday)**
 - Characterization of the background surface at the time of the overpass: use of GMI low frequency channels and T_{2m} for identification of different sea ice and snow cover;
 - Look-up tables built upon the results of this study (based on environmental variables, and surface type, ΔTB at 166 GHz and 183.3 GHz) to determine probability of snowfall.
- Use of regression tree analysis for other target variables (e.g., 183.3 ΔTB , 166 GHz TBs)
- Use the GMI/CPR snowfall dataset to assess GPROF V4 and V5 snowfall retrieval quality (similarly to what done for DPR products in *Casella et al., 2017*)
- Extend study to other radiometers (i.e., ATMS)

Future work: improve snowfall detection in H SAF PMW products

- Global PMW precipitation retrieval algorithms for GMI (H SAF product H20) (currently using ancillary T_{2m} for phase determination);
- Day-1 global products for EPS-SG MWI and MWS (CDOP-3)

H SAF: <http://hsaf.meteoam.it>

References

Casella, D., et al., Evaluation of the GPM-DPR snowfall detection capability: comparison with CloudSat, *Atmos. Res.*, 197, 64-75, doi :10.1016/j.atmosres.2017.06.018, 2017.

Casella D. et al., The Cloud Dynamics and Radiation Database algorithm for AMSR2: exploitation of the GPM observational dataset for operational applications, *IEEE J. of Sel. Topics in Appl. Earth Obs. and Rem. Sens. (J-STARS)*, 10(8), DOI : 10.1109/JSTARS.2017.2713485, 2017.

Ciabatta L., Marra A. C., Panegrossi G., Casella D., Sanò P., Dietrich S., Massari C., Brocca L., Daily precipitation estimation through different microwave sensors: Verification study over Italy, *J. of Hydrology*, 545, 436-450, doi: 10.1016/j.jhydrol.2016.12.057, 2017.

Panegrossi, G., et al.. T, H-SAF Federated Activity (H_SAF_FA15_01) “Cooperation on the use of combined spaceborne active and passive MW observations for precipitation retrieval”, Mid Term Report, Dec. 2016, pp.41

Panegrossi G., et al.: Use of the GPM constellation for monitoring heavy precipitation events over the Mediterranean region, *IEEE J. of Sel. Topics in Appl. Earth Obs. and Rem. Sens. (J-STARS)*, Volume 9, Issue 6, Pages: 2733 - 2753, doi: 10.1109/JSTARS.2016.2520660, 2016

Panegrossi et al., CloudSat-based assessment of GPM Microwave Imager snowfall observation capabilities , *Rem. Sensing*, submitted.

Sanò, P., et al.: The new Passive microwave Neural network Precipitation Retrieval (PNPR) algorithm for the cross-track scanning ATMS radiometer: description and verification study over Europe and Africa using GPM and TRMM spaceborne radars, *Atmos. Meas. Tech.*, 9, 5441-5460, doi:10.5194/amt-9-5441-2016, 2016